Learning Sequences of Manipulation Primitives for Robotic Assembly

Nghia Vuong[1], Hung Pham[2], and Quang-Cuong Pham[1,2]

***Abstract*— This paper explores the idea that skillful assembly is best represented as dynamic sequences of Manipulation Primitives, and that such sequences can be automatically discovered by Reinforcement Learning. Manipulation Primitives, such as "Move down until contact", "Slide along x while maintaining contact with the surface", have enough complexity to keep the search tree shallow, yet are generic enough to generalize across a wide range of assembly tasks. Policies are learned in simulation, and then transferred onto the physical platform. Direct sim2real transfer (without retraining in real) achieves excellent success rates on challenging assembly tasks, such as round peg insertion with 100 micron clearance or square peg insertion with large hole position/orientation estimation errors.**

I. INTRODUCTION

This paper explores the idea that skillful assembly is best represented as dynamic sequences of Manipulation Primitives, and that such sequences can be automatically discovered by Reinforcement Learning.

In recent years, increasingly complex assembly tasks have been demonstrated on robot systems [1]. However, in most cases, the difficult assembly skills, such as tight pin insertion or part mating, are still accomplished by hand-designed, hard-coded, strategies (e.g. spiral search followed by force-controlled insertion) [2]. Designing and fine-tuning such strategies require considerable engineering expertise and time, thus putting a brake on the deployment of intelligent robotic manipulation in the factories and in the homes. This paper investigates how to automatically discover *in silico* assembly strategies that robustly transfer to physical robots.

Representation of assembly skills as sequences of Manipulation Primitives

The first, crucial, question is the representation of the assembly skills: what is the set of atomic actions to be reasoned upon? In [3], the authors consider very simple atomic actions such as pure force-controlled translations or pure position-controlled rotations. This results in extremely long sequences of atomic actions to achieve a given task, making the search complexity overwhelming.

Consider how a robot would learn to play chess. One option is to learn directly the sequences of robot commands to physically move the pieces throughout the full game. Alternatively, it would be much more efficient to learn the sequences of piece moves (e.g. 1. e4, 2. Nf3, 3. Bb5...), and then rely on grasp planning, inverse kinematics, inverse dynamics, etc. to physically realize the moves.

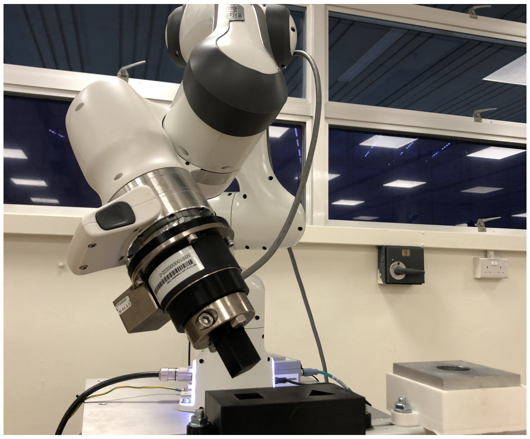

Fig. 1. Robotic assembly setup.

Here, we propose, by analogy, to consider Manipulation Primitives (MP) [4] as the atomic actions. Manipulation Primitives, such as "Move down until contact", "Slide along x while maintaining contact with the surface", have enough complexity to keep the search tree shallow (typically a sequence of 6 to 8 MPs is enough to achieve tight insertion), yet are generic enough to generalize across a wide range of assembly tasks (peg insertion with different peg shapes, large hole estimation errors, random initial positions...) Another key advantage of MPs is their additional *semantics*, which make them robust in sim2real and against model/environment variations and uncertainties: consider how "Move down until contact" is inherently more robust than a sequence of several short "Move down" actions.

Contribution: learning dynamic sequences of Manipulation Primitives

In [4], the authors consider a set of MPs with tunable parameters, the parameters being optimized through task execution on the physical platform. However, the *temporal sequence* of MPs to accomplish a given task is manually designed and fixed, which re-raises the initial concern about expertise and time required to address new tasks.

By contrast, we propose here to *automatically discover dynamic sequences* of MPs by Reinforcement Learning (RL). Policies are learned in simulation, and then transferred onto the physical platform. We show that direct sim2real transfer (without retraining in real) achieves 100% success rate on round peg insertion with 100 μm clearance and despite 0.5 mm and 0.5 deg errors in hole position/orientation estimation. On the harder task of square peg insertion with 1 mm clearance, 1.5 mm and 1.5 deg errors in hole

[1] Singapore Centre for 3D Printing (SC3DP), School of Mechanical and Aerospace Engineering, NTU, Singapore

[2] Eureka Robotics, Singapore

position/orientation estimation, direct sim2real transfer still achieves 75% success rate.

The rest of the paper is organized as follows. In Section II, we review works that are related to our proposed approach. In Section III, we formally define the Manipulation Primitives. In Section IV, we introduce in detail the proposed Reinforcement Learning formulation. In Section V, we present the experimental setup and quantitative results. Finally, in Section VI, we discuss the advantages and limitations of the presented approach, as well as some directions for future work.

II. RELATED WORK

Manipulation Primitives in robotic assembly. Manipulation primitive or skill primitive is a well-known concept in robot manipulation. An advantage of programming with manipulation primitives is to ”move beyond the low-level representations of the robot’s movements (classically joint-space or task-space and enable generalizing robot capabilities in terms of elemental actions that can be grouped together to complete any task” [2]. Recently, Johannsmeier et al. [4] represents an assembly skill as a directed graph whose nodes are MPs. They show that with the optimized parameters, the graph efficiently performs several cylindrical peg-in-hole tasks, even faster than human. However, the MPs are designed manually, thus lack the ability to generalize to different contexts. Furthermore, since the graph is generated offline, it could not adapt to environmental uncertainties that might occur during execution: one failure of any MPs might lead to the failure of the whole execution. In our method, we do not assume a fixed sequence of MPs; instead, the MP is generated at runtime.

Deep RL in high precision robotics assembly. Since high-precision assembly is a challenging task, making reinforcement learning tractable in this context requires careful design and consideration. In the following discussion, we review various ways reinforcement learning is made tractable in the context of high-precision assembly.

One technique that has been successfully applied to high-precision assembly task is smart action space discretization and problem decomposition. In [3], Inoue et al. decompose the task into a search phase and an insertion phase, and designs different state space, action space, and reward function for each phase. More specifically, several meta-actions are designed to form a discrete action space. This greatly speeds up training and achieves good performance at the same time. However, one drawback of this method is flexibility, since a few meta-actions limit the dynamic capabilities of the robot. We address this problem by using a large set of such meta-actions. Although this choice compromises the reduced training time, we adopt sim2real to address this issue and argue that the use of MPs as meta-actions makes the sim to real transfer more efficient. In the same vein, Hamaya et al. [5] divide the peg-in-hole task into five steps with different action spaces and state spaces. This decomposition greatly speeds up training through dimensional reduction of action and state spaces. The method, however, assumes a fixed sequence of steps that might not generalize well to other tasks.

In [6], Luo et al. combines iterative Linear-Quadratic-Gaussian (iLQG) [7] with an operational space force controller to learn local control policies, then train a neural network that generalizes this controller to adapt to environmental variations, taking into account the force feedback. This method is fast, being able to find a good control policy in just a few interactions, but relies on iLQG to find the local controllers that might not achieve a good performance on complex tasks, e.g. tight insertion tasks, due to the imposed linear structure on the system dynamic.

In [8], Schoettler et al. study the use of image observations and natural sparse rewards in several connector insertion tasks. They also compare two techniques for incorporating prior knowledge in RL: residual policy learning [9] and using demonstrations to guide the exploration of the subsequent RL algorithm. Furthermore, they reduce the dimensions of the action space: an action is a 3-dimensional position command. This implies that the parts are aligned in the first place, which make the task much easier. In fact, including orientation command results in interesting strategies, as can be seen in our experimental results.

One line of research utilizes sim to real (sim2real) transfer to reduce learning time on the real robot. Recent studies demonstrate impressive sim2real results in the context of high-precision assembly task. [10] applies system identification to align the several simulation parameters (gravity, joint damping, etc.) with the real robot dynamics. In [11], a meta RL algorithm called probabilistic embedding for actor-critic RL (PEARL) [12] is applied to learn the task structure for a family of related tasks in simulation and adapt quickly to a real task with few training data. Beltran et al. [13] use residual policy learning in combination with domain randomization.

III. MANIPULATION PRIMITIVES

A. Definition

We follow [4] to define manipulation primitives (MPs). An MP represents a desired motion of the robot end-effector (E) in the task frame (T). More precisely, it consists of:

- a desired velocity command ${}^{T}\mathbf{v}_{E}$ (in short $\mathbf{v}_{\mathrm{des}}$);
- a desired force command ${}^{T}\mathbf{f}_{E}$ (in short $\mathbf{f}_{\mathrm{des}}$);
- a stopping condition λ.

The desired velocity and force commands are defined as

$$\begin{aligned} \mathbf{v}_{\mathrm{des}}(t) &:= g_v(t, \boldsymbol{\Omega}_t; \boldsymbol{\theta}_v), \\ \mathbf{f}_{\mathrm{des}}(t) &:= g_f(t, \boldsymbol{\Omega}_t; \boldsymbol{\theta}_f), \end{aligned} \tag{1}$$

where g_v and g_f are any functions parameterized respectively by $\boldsymbol{\theta}_v$ and $\boldsymbol{\theta}_f$, and $\boldsymbol{\Omega}_t$ is the vector of all sensor signals at time t. Finally, the stopping condition is defined as $\lambda : (t, \boldsymbol{\Omega}_t) \mapsto \{\texttt{SUCCESS}, \texttt{FAILURE}, \texttt{CONTINUE}\}$. The next section instantiates our definition in the context of peg-in-hole insertion tasks and clarifies the motivations.

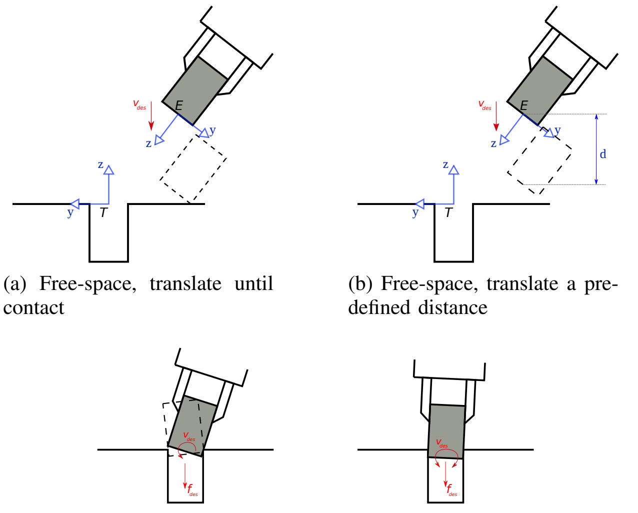

(a) Free-space, translate until contact

(b) Free-space, translate a predefined distance

(c) In-contact, rotate until next contact

(d) In-contact, insert

Fig. 2. Examples of Manipulation Primitives for insertion task. See text for details.

B. MPs for peg-in-hole insertion tasks

For insertion tasks, we consider two families of MPs: free-space MPs and in-contact MPs:

- Free-space MPs are to be executed when the robot is not in contact with the environment, i.e., when all external forces/torques are zero. MPs in this family are then associated with zero desired force/torque command.
- In-contact MPs are to be executed when the robot is in contact with the environment, i.e. when some of the external force/torque components are non-zero. In addition to other objectives, MPs in this family have some of the components of their desired force/torque command to be non-zero in order to maintain the same contact state during the execution.

Each family of MPs are sub-divided into several types: (i) move until (next) contact, (ii) move a predefined amount, (iii) insert. Figure 2 illustrates some examples of MPs, which are further detailed below. The set of all 91 MPs that are used in our experiments is given in Table I.

Free-space, move until contact. Translate the end-effector along a direction, or rotate the end-effector about a direction, until contact is detected. The example of (Fig. 2a) translates the end-effector in the $-z$ direction with speed v until the measured force is larger than f_{thr} (SUCCESS), or $t > 2s$ (FAILURE), which is formally defined by

$$\begin{aligned}
\mathbf{v}_{\text{des}}(t) &= [0,0,-v,0,0,0] \\
\mathbf{f}_{\text{des}}(t) &= \mathbf{0} \\
\lambda(t) &= \begin{cases} \texttt{SUCCESS} & \text{if } \mathbf{f}_{\text{ext}}^T \mathbf{u}_v > f_{\text{thr}}, \\ \texttt{FAILURE} & \text{if } t > 2, \\ \texttt{CONTINUE} & \text{otherwise.} \end{cases}
\end{aligned} \tag{2}$$

where $\mathbf{f}_{\text{ext}}$ is the measured external force, $\mathbf{u}_v = \mathbf{v}_{\text{des}}/||\mathbf{v}_{\text{des}}||$ is the moving direction.

Free-space, move a predefined amount. Translate the end-effector along a direction over a predefined distance d, or rotate about a direction over a predefined angle α. The example of (Fig. 2b) translates the end-effector in the $-z$ direction with speed v, until the distance d is reached (SUCCESS), or a large contact force is detected (FAILURE), which is formally defined by

$$\begin{aligned}
\mathbf{v}_{\text{des}}(t) &= [0,0,-v,0,0,0] \\
\mathbf{f}_{\text{des}}(t) &= \mathbf{0} \\
\lambda(t) &= \begin{cases} \texttt{SUCCESS} & \text{if } \Delta\mathbf{p}^T \mathbf{u}_v > d \\ \texttt{FAILURE} & \text{if } \mathbf{f}_s^T \mathbf{u}_v > f_{\text{thr}} \\ \texttt{CONTINUE} & \text{otherwise} \end{cases}
\end{aligned} \tag{3}$$

where $\Delta\mathbf{p}$ is the distance between the current pose $\mathbf{p}$ and the start pose $\mathbf{p}_0$.

In-contact, move until next contact. Track a non-zero force in a some directions, and translate the end-effector along a direction, or rotate the end-effector about a direction until next contact is detected. The example of Fig 2c control a force f_d in the $-z$ direction and rotate the peg around the x direction with speed v, until the measured force is larger than f_{thr} (SUCCESS), or $t > 2s$ (FAILURE), which is formally defined as

$$\begin{aligned}
\mathbf{v}_{\text{des}}(t) &= [0,0,0,0,v,0] \\
\mathbf{f}_{\text{des}}(t) &= [0,0,-f_d,0,0,0] \\
\lambda(t) &= \begin{cases} \texttt{SUCCESS} & \text{if } \mathbf{f}_{\text{ext}}^T \mathbf{u}_v > f_{\text{thr}}, \\ \texttt{FAILURE} & \text{if } t > 2, \\ \texttt{CONTINUE} & \text{otherwise.} \end{cases}
\end{aligned} \tag{4}$$

In-contact, insert. Track a non-zero force in the direction of insertion and regulate the forces and torques to zero in all the other directions. The example of (Fig. 2d) performs the insertion in the z direction, as formally defined by

$$\begin{aligned}
\mathbf{v}_{\text{des}}(t) &= -K_d \mathbf{f}_{\text{ext}} \\
\mathbf{f}_{\text{des}}(t) &= [0,0,f_d,0,0,0] \\
\lambda(t) &= \begin{cases} \texttt{SUCCESS} & \text{if } d(\mathbf{p},\mathbf{p}_t) < \epsilon \\ \texttt{FAILURE} & \text{if } t > 2 \\ \texttt{CONTINUE} & \text{otherwise} \end{cases}
\end{aligned} \tag{5}$$

where K_d is a compliant 6×6 diagonal matrix, $d(.)$ is a metric measuring distance between two poses, $\mathbf{p}_g$ is the goal pose. For simplicity, we consider a diagonal compliant matrix of the form $K_d = \begin{bmatrix} k_{dt}\mathbb{I}^{3\times3} & \mathbf{0} \\ \mathbf{0} & k_{dr}\mathbb{I}^{3\times3} \end{bmatrix}$.

IV. LEARNING DYNAMIC SEQUENCES OF MANIPULATION PRIMITIVES BY RL

The MPs sequencing problem is to find sequences in a finite set $\mathbb{M}$ of MPs that successfully perform a particular task. More specifically, we are interested in the family of insertion tasks, which is characterized by a goal configuration.

TABLE I

THE SET OF 91 MANIPULATION PRIMITIVES USED IN OUR EXPERIMENTS.

Family	Type	Axis	Parameters	Values	N
Free space	Translate until contact (T^c)	$-z$	v f_{thr}	10 mm/s 8 N	1
	Translate (T)	$\pm x, \pm y, \pm z$	v f_{thr} d	10 mm/s 15 N 2 or 4 mm	12
	Rotate (R)	$\pm x, \pm y, \pm z$	v f_{thr} d	9 deg/s 1 Nm 2 or 4 deg	12
In contact	Translate until next contact (T^c)	$\pm x, \pm y$	v f_{thr} f_d	4 or 7.5 mm/s 8 or 15 N -3 N	16
	Rotate until next contact (R^c)	$\pm x, \pm y, \pm z$	v f_{thr} f_d	4 or 7 deg/s 0.1 or 0.5 Nm -3 N	24
	Translate (T)	$\pm x, \pm y$	v f_{thr} d f_d	10 mm/s 15 N 2 or 4 mm -3 N	8
	Rotate (R)	$\pm x, \pm y, \pm z$	v f_{thr} d f_d	4.6 deg/s 1 Nm 2 or 4 deg -3 N	12
	Insert (I)	$-z$	ϵ k_{dt} k_{dr} f_d	2mm 0.01 0.05 or 0.1 -5 or -12 N	4

A. Overview of Reinforcement Learning

We consider here the discounted episodic RL problem. In this setting, the problem is described as a Markov Decision Process (MDP) [14]. At each time step t, the agent observes current state $\mathbf{s}_t \in \mathbb{S}$, executes an action $\mathbf{a}_t \in \mathbb{A}$, and receives an immediate reward r_t. The environment evolves through the state transition probability $p(\mathbf{s}_{t+1}|\mathbf{s}_t, \mathbf{a}_t)$. The goal in RL is to learn a policy $\mathbf{a}_t = \pi(\mathbf{s}_t)$ that maximizes the expected discounted return $R = \sum_{t=1}^{T} \gamma^t r_t$, where γ is the discount factor that tends to emphasize the importance of most recent rewards.

B. Our RL setting

State and action. An action is the index of an MP to be executed. This results in a discrete action space since the MP set $\mathbb{M}$ contains a finite number of MPs. This action set consists of two subspaces: $\mathbb{A}_{\text{free}}$ containing all free-space MPs and $\mathbb{A}_{\text{con}}$ containing all in-contact MPs. We define the state vector $\mathbf{s}_t = [\mathbf{p}(t), \mathbf{f}_{ext}(t)]$. where $\mathbf{p}$ is the relative pose between the two involved parts, computed from the joint position, the goal pose, and forward kinematics; $\mathbf{f}_{ext}$ is the external force and torque acting on the end-effector. All of the measurement and calculation at time t are performed after the execution of the MP at time $t-1$, i.e. the stop condition λ returns `SUCCESS` or `FAILURE`. The set of feasible actions at each state $\mathbf{s}_t$ is either $\mathbb{A}_{\text{free}}$ if $\mathbf{f}_{\text{ext}} = \mathbf{0}$, or $\mathbb{A}_{\text{con}}$ if $\mathbf{f}_{\text{ext}} \neq \mathbf{0}$.

Algorithm and policy parameterization. We use Proximal Policy Optimization (PPO) [15], an on-policy and model-free RL algorithm. The policy and value function are represented by neural networks. Due to its noisy nature, we do not use force measurement as the input to the policy and value functions. The value function is a Multilayer Perceptron (MLP). For the policy, we use two separate neural networks for each of the action subspace, which is illustrated in Fig. 3

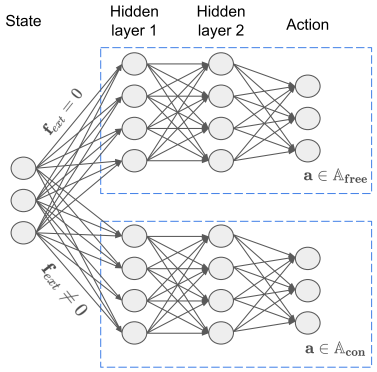
State
Hidden layer 1
Hidden layer 2
Action
$\mathbf{f}_{ext} = 0$
$\mathbf{f}_{ext} \neq 0$
$\mathbf{a} \in \mathbb{A}_{\text{free}}$
$\mathbf{a} \in \mathbb{A}_{\text{con}}$

Fig. 3. Neural network architecture for our RL setting.

Reward function. We define the reward function as

$$r(\mathbf{o}_t, \mathbf{o}_{t+1}, \mathbf{a}_t) := c_1 \left(e^{\frac{-||\mathbf{p}_{t+1} - \mathbf{p}_{goal}||_2^2}{k_1}} - 1 \right) - c_2 t(\mathbf{a}_t) + c_3 s(\mathbf{a}_t) \tag{6}$$

The first term rewards for moving closer to the goal, the second term is the execution time of the MP, to bias the algorithm to find solution with short execution time. The third term $s(\mathbf{a}_t) = 0$ if a `SUCCESS` status is returned, $s(\mathbf{a}_t) = -1$ if a `FAILURE` status is returned.

TABLE II

DIMENSIONS AND MATERIAL OF PEGS AND HOLES

Profile	Hole size	Insertion depth	Material	Clearance
Round	30 mm	20 mm	Aluminum	0.1 mm
Square	20.5 mm	20 mm	Plastic	1 mm
Triangle	25.1 mm	29 mm	Plastic	1 mm

V. EXPERIMENTS

A. System description

Task description. We design multiple peg-in-hole tasks with three types of peg profiles: round shape, square shape, and triangular shape. The properties of the pegs are shown in Table II We make the following assumptions regarding the insertion tasks: (1) The peg is firmly mounted to the robot end-effector (2) The hole is fixed in the environment (3) An estimation of the relative position and orientation between the peg and hole can be obtained, either by a vision system or by teaching.

Robot system setup. A 7-DOF Franka Emika Panda cobot is used in our experiment. We use the Mujoco physics engine [16] and adapt an open-source Panda robot model [1]. The controller is simulated with a control frequency of 500Hz. In real world, we additionally use a Gamma IP60 force torque sensor to measure the external force acting on the end-effector. The measurement from FT sensor is needed to implement insert primitive, as the external force estimation in `libfranka` is not precise enough to perform this primitive. We teach the position of the hole for real world experiments

Implementation details. We use `gym` [17] to design the environment and `rlpyt` [18], a RL framework based on PyTorch for the implementation of PPO algorithm.

B. Training in simulation

We design the environments in Mujoco for three peg-in-hole tasks with different peg and hole shapes: round, square and triangle. The default starting position of the peg is above the hole 10 mm. To improve the robustness and generalization capability of the trained policy, at the start of each episode, we add a displacement $\Delta\mathbf{p}_{\text{init}}$ to the starting position and hole estimation error $\Delta\mathbf{p}_{\text{hole}}$ to the true hole pose. For each task, we train on two different Training Conditions:

(TC1) $\Delta\mathbf{p}_{\text{init}}$ is uniformly sampled in $(-1, 1)$ mm for position and in $(-1, 1)$ deg for orientation, $\Delta\mathbf{p}_{\text{hole}} = \mathbf{0}$;

(TC2) $\Delta\mathbf{p}_{\text{init}}$ is uniformly sampled in $(-2, 2)$ mm for position and $(-2, 2)$ deg for orientation, $\Delta\mathbf{p}_{\text{hole}}$ is uniformly sampled in $(-1, 1)$ mm for position and in $(-1, 1)$ deg for orientation,

The weights of the policy trained for (TC1) is used to initialize the policy trained with (TC2). We do not train directly on (TC2) due to its difficulty. The success rate and average reward during training are reported in Fig. 4.

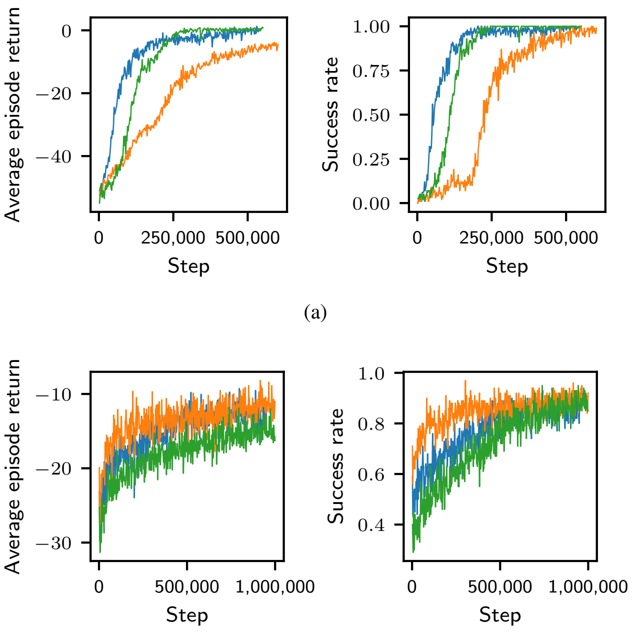

(a)

(b)

Fig. 4. Training curve (average episode reward and success rate) for (a) Training Condition TC1 and (b) Training Condition TC2.

C. Sim2real policy transfer on physical robot

We evaluate the learned policies directly on the real robot without any further fine-tuning. The results are reported in Fig 6. We consider three Evaluation Conditions:

(EC1) Nominal performance: $\Delta\mathbf{p}_{\text{init}}$ is sampled in $(-0.5, 0.5)$ mm for position and in $(-0.5, 0.5)$ deg for orientation, $\Delta\mathbf{p}_{\text{hole}} = \mathbf{0}$;

(EC2) Generalizability: $\Delta\mathbf{p}_{\text{init}}$ is sampled in $(-0.5, 0.5)$ mm for position and in $(-0.5, 0.5)$ deg for orientation, $\Delta\mathbf{p}_{\text{hole}} = \mathbf{0}$;

(EC3) Robustness: $\Delta\mathbf{p}_{\text{init}}$ is sampled in $(-1, 1)$ mm for position and $(-1, 1)$ deg for orientation, $\Delta\mathbf{p}_{\text{hole}}$ is sampled in $(-1.5, 1.5)$ mm for position and in $(-1.5, 1.5)$ deg for orientation

Different from the training phase, the hole estimation error and the initial pose displacement are sampled on the *boundary* of the box around the norminal values.

We next compare the transfer result with a manually-defined sequence of MPs and report the result in Fig 6. This sequence is tuned for the round peg-in-hole task with an estimation error of 1 mm in translation and 1 deg in orientation. More specifically, the sequence is (1) rotate about $-y$ 5 deg; (2) translate along $-z$ until next contact; (3) translate along x until next contact; (4) rotate about y until next contact; (5) insert. One can see that the manually-defined solution does not generalize well: for both round and square tasks, the success rates for Evaluation Condition EC2 are significantly lower than our proposed method.

We also run the trained policy on tasks with different shapes from the one the policy was trained for, on $N = 10$ trials. The results are shown in Fig 7. The result demonstrates the generalization capability of the trained policy across

[1] available online at franka_sim

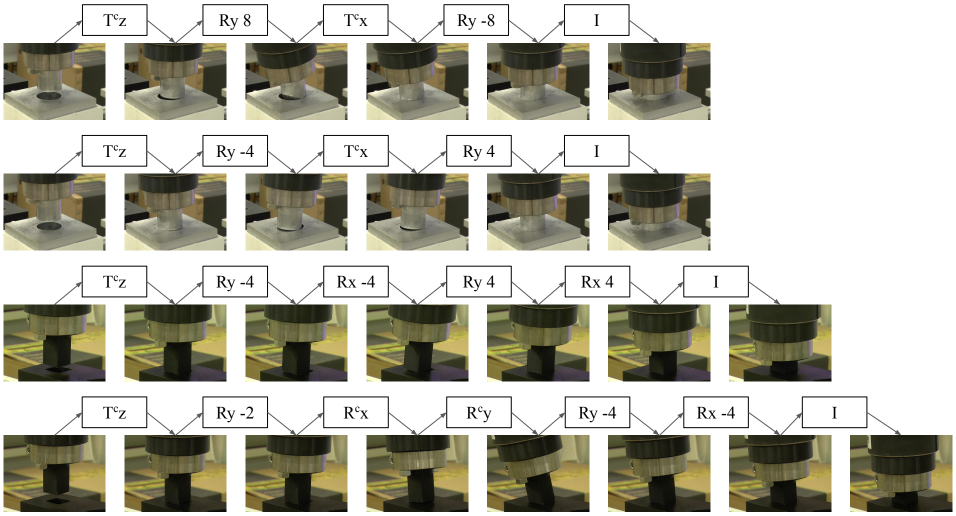

Fig. 5. Snapshots of four runs on the round and square peg-in-hole insertion tasks. "Ry 8" means rotation of 8 deg around y, which is the concatenation of two MPs that rotate 4 deg each. Note the different sequences of MPs for the same task, which illustrates the *dynamic* character of the learned policies.

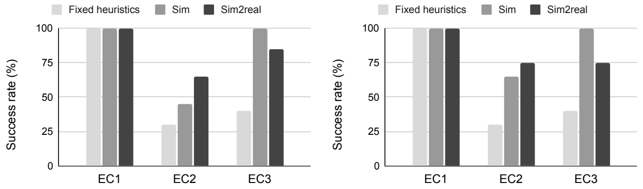

(a) Round

(b) Square

Fig. 6. Evaluation on the round and square peg-in-hole task on three Evaluation Conditions.

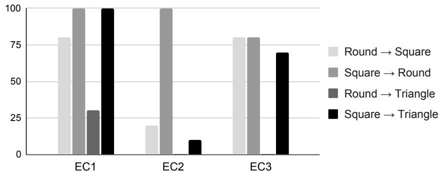

Fig. 7. Results for the policy transfer experiments. $A \rightarrow B$: the policy trained for shape A is evaluated on shape B.

different geometries of the parts. For instance, the policy trained for square peg-in-hole confidently solves the round peg-in-hole task, even with large estimation error.

D. Dynamic character of the learned policies

We investigate next the emergent behaviors exhibited by the trained policies. All strategies tend to find a correct pose, such that the insert MP could completes the task afterward. To achieve such pose, the most commonly used MP is of rotation type, as can be seen in Fig. 5. Rotating motion induces a tilted peg posture. This posture effectively broadens the state spaces in which parts of the peg are inside the hole. Interestingly, for the square peg-in-hole task, the policy follows this strategy by rotating the peg in both x and y directions. After reaching such states, a "translate until contact" often comes next to achieves the locally "optimal" position, where the peg is at the lowest position (refer to two top rows of Fig. 5). After that, a rotating motion is regulated to cancel the one in previous steps, before the insertion takes place.

VI. CONCLUSIONS

In this paper, we have explored the idea that skillful assembly is best represented as dynamic sequences of Manipulation Primitives, and that such sequences can be automatically discovered by Reinforcement Learning. To illustrate this idea, we designed a set of MPs for peg-in-hole insertion tasks, and proposed a sim2real approach: policies are learned in simulation, and then transferred onto the physical platform, without re-training in real. The experimental results showed that policies learned purely in simulation were able to consistently solve tight-clearance round peg insertion tasks, and square peg insertion tasks with large estimation errors.

In future work, we shall evaluate our approach on more complex tasks, such as a tight-clearance polygonal peg-in-hole insertion, multiple pin insertion, connector insertion, gear assembly, DIMM memory assembly, etc.

Another potential direction is to integrate tactile and visual information, either to select the correct next MP, or to design a visual-based MP, such as "visual servoing".

In tasks that have complex dynamics, where instability is a key consideration, the choice of the low-level control law in each MPs define the upper limit of the overall system performance. Hence, incorporating advanced robust control laws [19] is a promising direction.

ACKNOWLEDGMENT

This research was supported by the National Research Foundation, Prime Ministrer's Office, Singapore under its Medium Sized Centre funding scheme, Singapore Centre for 3D Printing, CES_SDC Pte Ltd, and Chip Eng Seng Corporation Ltd.

References

[1] F. Suárez-Ruiz, X. Zhou, and Q.-C. Pham, "Can robots assemble an ikea chair?" *Science Robotics*, vol. 3, no. 17, 2018.

[2] F. Suárez-Ruiz and Q.-C. Pham, "A framework for fine robotic assembly," in *2016 IEEE international conference on robotics and automation (ICRA)*. IEEE, 2016, pp. 421–426.

[3] T. Inoue, G. De Magistris, A. Munawar, T. Yokoya, and R. Tachibana, "Deep reinforcement learning for high precision assembly tasks," in *2017 IEEE/RSJ International Conference on Intelligent Robots and Systems (IROS)*. IEEE, 2017, pp. 819–825.

[4] L. Johannsmeier, M. Gerchow, and S. Haddadin, "A framework for robot manipulation: Skill formalism, meta learning and adaptive control," in *2019 International Conference on Robotics and Automation (ICRA)*. IEEE, 2019, pp. 5844–5850.

[5] M. Hamaya, R. Lee, K. Tanaka, F. von Drigalski, C. Nakashima, Y. Shibata, and Y. Ijiri, "Learning robotic assembly tasks with lower dimensional systems by leveraging physical softness and environmental constraints," in *2020 IEEE International Conference on Robotics and Automation (ICRA)*. IEEE, 2020, pp. 7747–7753.

[6] J. Luo, E. Solowjow, C. Wen, J. A. Ojea, A. M. Agogino, A. Tamar, and P. Abbeel, "Reinforcement learning on variable impedance controller for high-precision robotic assembly," in *2019 International Conference on Robotics and Automation (ICRA)*. IEEE, 2019, pp. 3080–3087.

[7] E. Todorov and W. Li, "A generalized iterative lqg method for locally-optimal feedback control of constrained nonlinear stochastic systems," in *Proceedings of the 2005, American Control Conference, 2005.* IEEE, 2005, pp. 300–306.

[8] G. Schoettler, A. Nair, J. Luo, S. Bahl, J. A. Ojea, E. Solowjow, and S. Levine, "Deep reinforcement learning for industrial insertion tasks with visual inputs and natural rewards," *arXiv preprint arXiv:1906.05841*, 2019.

[9] T. Johannink, S. Bahl, A. Nair, J. Luo, A. Kumar, M. Loskyll, J. A. Ojea, E. Solowjow, and S. Levine, "Residual reinforcement learning for robot control," in *2019 International Conference on Robotics and Automation (ICRA)*. IEEE, 2019, pp. 6023–6029.

[10] M. Kaspar, J. D. M. Osorio, and J. Bock, "Sim2real transfer for reinforcement learning without dynamics randomization," *arXiv preprint arXiv:2002.11635*, 2020.

[11] G. Schoettler, A. Nair, J. A. Ojea, S. Levine, and E. Solowjow, "Meta-reinforcement learning for robotic industrial insertion tasks," *arXiv preprint arXiv:2004.14404*, 2020.

[12] K. Rakelly, A. Zhou, C. Finn, S. Levine, and D. Quillen, "Efficient off-policy meta-reinforcement learning via probabilistic context variables," in *International conference on machine learning*, 2019, pp. 5331–5340.

[13] C. C. Beltran-Hernandez, D. Petit, I. G. Ramirez-Alpizar, and K. Harada, "Variable compliance control for robotic peg-in-hole assembly: A deep-reinforcement-learning approach," *Applied Sciences*, vol. 10, no. 19, p. 6923, 2020.

[14] R. S. Sutton and A. G. Barto, *Reinforcement learning: An introduction*. MIT press, 2018.

[15] J. Schulman, F. Wolski, P. Dhariwal, A. Radford, and O. Klimov, "Proximal policy optimization algorithms," *arXiv preprint arXiv:1707.06347*, 2017.

[16] E. Todorov, T. Erez, and Y. Tassa, "Mujoco: A physics engine for model-based control," in *2012 IEEE/RSJ International Conference on Intelligent Robots and Systems*. IEEE, 2012, pp. 5026–5033.

[17] G. Brockman, V. Cheung, L. Pettersson, J. Schneider, J. Schulman, J. Tang, and W. Zaremba, "Openai gym," *arXiv preprint arXiv:1606.01540*, 2016.

[18] A. Stooke and P. Abbeel, "rlpyt: A research code base for deep reinforcement learning in pytorch," *arXiv preprint arXiv:1909.01500*, 2019.

[19] H. Pham and Q.-C. Pham, "Convex controller synthesis for robot contact," *IEEE Robotics and Automation Letters*, vol. 5, no. 2, pp. 3330–3337, 2020.